RESEARCH ARTICLE

Multimode Interferometers: an Analytical Method for Determining the Accumulated Phase Difference Between the Fundamental Mode and One Arbitrary High-Order Mode

Yuri Hayashi Isayama^a

^a Department of Physics, Federal University of Minas Gerais, Av. Presidente Antônio Carlos, 6627, Belo Horizonte, Minas Gerais, Brazil.

ARTICLE HISTORY

Compiled September 5, 2024

ABSTRACT

In multimode interferometers, the interaction between several modes brings a high level of complexity to the interpretation of its light patterns. With recent advances, it is possible to selectively excite only a couple of modes inside the device. This paper presents an analytical method for determining the phase difference between two propagating modes in the multimode interferometer, in an effort to simplify the usage and expand the range of applications for this type of optical devices.

KEYWORDS

Integrated optics; Optical Waveguides; Multimode Interference; Optical

Interferometry; Photonics

1. Introduction

Interferometers represent one fundamental building block in the field of integrated optics. Its applications can vary in a wide range, such as switches and modulators [1], optical logic gates [2], and optical sensors [3–5]. One type of interferometer is the Multimode Interferometer (MMI). In this structure, light is distributed among different optical modes that travel with different propagation constants. At the end of the MMI, the light pattern observed depends on the different phases accumulated by the modes throughout the propagation distance. This working mechanism has been widely used in recent years in sensing applications [6–9]. The sensitivity of the device has been improved through different approaches, such as: coupling structures to improve light coupling to the optical modes [9–11], engineering of the waveguide core to enhance the interaction between light and matter [12], and the use of high-order modes [13–15] and different polarizations (TE/TM) [16,17]. The introduction of higher-order modes can drastically improve device sensitivity, but the interaction between the modes also becomes much more complex. One solution is to reduce the number of propagating modes within the MMI with new coupling structures, as presented in [14], but the interpretation of the output light is not straightforward. In this paper, an analytical method for determining the phase difference between the fundamental mode (both

TE or TM) and an arbitrary high-order (order n) mode at the end of the MMI is presented.

2. Mathematical Modeling

A MMI is basically composed of three sections: an input section, which is responsible for exciting the different propagating modes within the MMI; a multimode waveguide (MMW), where all the excited modes propagate through a certain distance; and an output section, where light is captured by a physical structure (such as another waveguide) or a detection instrument (photodetector, photodetector array, CCD camera, etc.). The analysis here presented concerns the multimode waveguide (MMW) section of the MMI.

2.1. Basic expression for optical power at the end of the MMW

Consider the multimode waveguide (MMW) section of a Multimode Interferometer (MMI) with a cross-section as shown in Figure 1. Inside the MMW (i.e. $|x| \leq W/2$), the m^{th} Transverse Electric (TE) mode has the following electric field distribution:

$$E_x^m(x,z) = A_m \cos\left(\frac{2u_m}{W}x - \frac{m\pi}{2}\right)e^{-j\beta_m z},\tag{1}$$

where E_x denotes the electric field in the x direction, m is the number of the mode $(m=0 \text{ represents the fundamental TE}_0 \text{ mode}, m=1 \text{ the TE}_1 \text{ mode, and so on}), <math>A_m$ is the amplitude of the m^{th} mode, W is the MMW core width, β_m is the propagation constant of the m^{th} mode, and $u_m \approx (m+1)\frac{\pi}{2}$ [18].

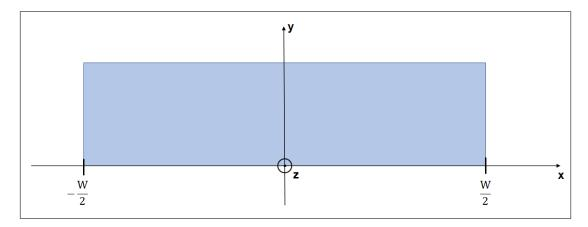


Figure 1. Cross-section of a multimode waveguide.

If there are solely two propagating modes in the MMW, TE_0 and TE_n , at the end of the MMW (i.e. $z = L_{MMI}$), the electric field distribution will be as follows:

$$E_x(x, L_{MMI}) = A_0 \cos\left(\frac{\pi}{W}x\right) e^{-j\beta_0 L_{MMI}} + A_n \cos\left(\frac{(n+1)\pi}{W}x - \frac{n\pi}{2}\right) e^{-j\beta_n L_{MMI}}.$$
(2)

The optical power is proportional to $|E_x^2|$, therefore

$$|E_x(x, L_{MMI})|^2 = \left| A_0 \cos\left(\frac{\pi}{W}x\right) e^{-j\phi_0} + A_n \cos\left(\frac{(n+1)\pi}{W}x - \frac{n\pi}{2}\right) e^{-j\phi_n} \right|^2, \quad (3)$$

with $\phi_{\alpha} = \beta_{\alpha} L_{MMI}$. Applying the law of cosines to expand Eq. 3, we obtain

$$|E_{x}(x, L_{MMI})|^{2} = A_{0}^{2} \cos^{2}\left(\frac{\pi}{W}x\right) + A_{n}^{2} \cos^{2}\left(\frac{(n+1)\pi}{W}x - \frac{n\pi}{2}\right) - 2A_{0}A_{n}\cos\left(\frac{\pi}{W}x\right)\cos\left(\frac{(n+1)\pi}{\pi}Wx - \frac{n\pi}{2}\right)\cos(\phi_{0} - \phi_{n}).$$
(4)

The TE_n mode presents maximum electric field intensity at the points

$$\frac{(n+1)\pi}{W}x - \frac{n\pi}{2} = \tau\pi, \tau \in \mathbb{Z}^- \cup \{0\}$$

$$x = \left(\tau + \frac{n}{2}\right) \frac{W}{n+1}, |x| \le \frac{W}{2}.\tag{5}$$

In each of these points, the optical power is given by:

$$\left| E_x \left(x = (\tau + \frac{n}{2}) \frac{W}{n+1}, z = L_{MMI} \right) \right|^2 =
= A_0^2 \cos^2 \left[(\tau + \frac{n}{2}) \frac{\pi}{n+1} \right] + A_n^2 \cos^2 \left[(\tau + \frac{n}{2}) \pi - \frac{n}{2} \pi \right] -
- 2A_0 A_n \cos \left[(\tau + \frac{n}{2}) \frac{\pi}{n+1} \right] \cos \left[(\tau + \frac{\pi}{2}) \pi - \frac{n\pi}{2} \right] \cos \Delta \phi, \quad (6)$$

with $\Delta \phi = \phi_0 - \phi_n$. Simplifying the arguments of cosines (and because $\cos^2[\tau \pi] = 1$), we arrive at

$$\left| E_x \left((\tau + \frac{n}{2}) \frac{W}{n+1}, L_{MMI} \right) \right) \right|^2 = A_0^2 \cos^2 \left(\frac{\tau + \frac{n}{2}}{n+1} \pi \right) + A_n^2 - 2A_0 A_n \cos \left(\frac{\tau + \frac{n}{2}}{n+1} \pi \right) \cos(\tau \pi) \cos \Delta \phi. \quad (7)$$

2.2. Some remarks on number of optical power peaks and their location

Assuming the following hypothesis: the number of optical power maxima is always equal to n+1. We defined $\tau \in \mathbb{Z}^- \cup \{0\}$ and $|x| < \frac{W}{2}$. If there were more optical maxima than n+1, then there should be a value of τ such as $\tau \leq -(n+1)$. The optical power maxima occur in the points

$$|x| = \left| \left(\tau + \frac{n}{2} \right) \frac{W}{n+1} \right| = \left| \tau + \frac{n}{2} \frac{W}{n+1} \right|, \tag{8}$$

since $n \ge 0$. If $\tau = -(n+1)$, then

$$\left|\tau + \frac{n}{2}\right| = -\left(\tau + \frac{n}{2}\right). \tag{9}$$

The power peak location corresponding to $\tau = -(n+1)$ is

$$|x| = -\left(\frac{-2(n+1)}{n+1}\right)\frac{W}{2} = W > \frac{W}{2}.$$
 (10)

Therefore, $\tau < -(n+1)$, $|x| > \frac{W}{2}$ and, thus, the number of maxima will always be n+1, with $\tau \in \{-n, -n+1, ..., 1, 0\}$.

Because of the symmetry of the MMW core, it is expected that the optical power peaks are located in symmetrical positions in relation to the plane x = 0. If there is a peak in $x = x_0$, there should be a symmetrical peak in $x = -x_0$ (except for the case of $x_0 = 0$, when there is a peak at the origin, which means the optical mode has even symmetry and an odd number of peaks – i.e. n = 2k + 1, $k \in \mathbb{Z}$).

Consider a MMW with a mode of order n (TE_n) and the pair of cases $\tau = 0$ and $\tau = -n$:

$$\tau = 0 \Rightarrow x = \left(\frac{n}{2}\right) \frac{W}{n+1} = \frac{n}{n+1} \frac{W}{2} = x_0$$

$$\tau = -n \Rightarrow x = \left(-n + \frac{n}{2}\right) \frac{W}{n+1} = \frac{-n}{n+1} \frac{W}{2} = x_n$$

which gives us $x_0 = x_n$.

If we expand this to the case $\tau = -k$ and $\tau = -(n-k)$:

$$\tau = -k \Rightarrow x = \left(-k + \frac{n}{2}\right) \frac{W}{n+1} = \left(\frac{-2k}{n+1} + \frac{n}{n+1}\right) \frac{W}{2} = x_k$$
 (11)

$$\tau = -(n-k) \Rightarrow$$

$$x = \left(-n+k+\frac{n}{2}\right)\frac{W}{n+1} = \left(\frac{2k}{n+1} - \frac{n}{n+1}\right)\frac{W}{2} = x_{n-k}. \quad (12)$$

The optical power peaks occur in pairs $(x_k \text{ and } x_{n-k})$ in terms of their position in the x axis, where for TE_n modes with even order $(n=2\alpha)$, there is an additional central peak. In the modes TE_n with odd order $(n=2\alpha+1)$, this central peak does not exist.

2.3. Developing an expression for the phase difference between the two propagating modes

Let us revisit Eq. 3:

$$|E_x(x,L_{MMI})|^2 = \left| A_0 cos\left(\frac{\pi}{W}x\right) e^{-j\phi_0} + A_n cos\left(\frac{(n+1)\pi}{W}x - \frac{n\pi}{2}\right) e^{-j\phi_n} \right|^2.$$

At the optical power peaks corresponding to $x = (\tau + \frac{n}{2}) \frac{W}{n+1}$, the argument of the second cosine in Eq. 3 shall assume values of $\frac{(n+1)\pi}{W}x - n\frac{\pi}{2} = \tau\pi$, with $\tau \in \mathbb{Z}^- \cup \{0\}$. Starting from $\tau = 0$ to $\tau = -n$, one may note that $\cos\left[\frac{(n+1)pi}{W}x - n\frac{\pi}{2}\right] = \cos(\tau\pi)$. The value of the cosine alternates between $\cos(0)$ and $\cos(\pi)$ for the different values of τ . The result is that for consecutive peaks, the value of $\cos\left[\frac{(n+1)pi}{W}x - n\frac{\pi}{2}\right]$ alternates between 0 and -1, and if $x_{\tau} = (\tau + \frac{n}{2}) \frac{W}{n+1}$, then we may say that

$$|E_x(x_\tau, L_{MMI})|^2 = \left| A_0 \cos\left(\frac{\pi}{W} x_\tau\right) e^{-j\phi_0} + A_n \cos\left(\frac{n+1}{W} x_\tau - n\frac{\pi}{2}\right) e^{-j\phi_n} \right|^2 =$$

$$= A_0^2 \cos^2\left(\frac{\pi}{W} x_\tau\right) + A_n^2 - 2A_0 A_n \cos\left(\frac{\pi}{W} x_\tau\right) \cos(\tau \pi) \cos\Delta\phi \quad (13)$$

and for $x = x_{\tau-1}$

$$|E_x(x_{\tau-1}, L_{MMI})|^2 = A_0^2 \cos^2\left(\frac{\pi}{W}x_{\tau-1}\right) + A_n^2 - 2A_0A_n\cos\left(\frac{\pi}{W}x_{\tau-1}\right)\cos(\tau\pi)\cos(\Delta\phi). \tag{14}$$

There are two cases that need to be analyzed: when the order n is odd and when it is even.

If n is odd: there is an even number of power peaks equal to n+1. If k is a natural number, then every peak represented by $\tau=k$ has its symmetrical $\tau=-(n-k)$. These symmetrical peaks are such that the term $2A_0A_n\cos\left(\frac{\pi}{W}x_k\right)\cos(\tau\pi)\cos\Delta\phi$ equals to $2A_0A_n\cos\left(\frac{\pi}{W}x_{n-k}\right)\cos(\tau\pi)\cos\Delta\phi$, since $x_k=-x_{n-k}$ (see Eqs. 11 and 12). Because the signal of such term is inverted for consecutive values of τ (see Eqs. 13 and 14), the existence of an even number of power peaks implies that the terms $2A_0A_n\cos\left(\frac{\pi}{W}x_k\right)\cos(\tau\pi)\cos\Delta\phi$ and $2A_0A_n\cos\left(\frac{\pi}{W}x_{n-k}\right)\cos(\tau\pi)\cos\Delta\phi$ will present opposite signs and, thus, we have

$$|E_x(x_k, L_{MMI})|^2 + |E_x(x_{n-k}, L_{MMI})|^2 = 2A_0^2 cos^2 \left(\frac{\pi}{W}x_k\right) + 2A_n^2$$
 (15)

If we add all the power peaks, the result will be

$$\sum_{\tau=0}^{n} |E_x(x_{\tau}, L_{MMI})|^2 = \sum_{\tau=0}^{n} \left[A_0^2 \cos^2 \left(\frac{\pi}{W} x_{\tau} \right) + A_n^2 \right], \tag{16}$$

which is independent from the value of $\Delta \phi$. On the other hand, if we subtract the power of symmetrical peaks:

$$|E_x(x_k, L_{MMI})|^2 - |E_x(x_{n-k}, L_{MMI})|^2 =$$

$$= -4A_0 A_n \cos\left(\frac{\pi}{W} x_k\right) \cos(k\pi) \cos\Delta\phi. \quad (17)$$

Performing the same sum of all pairs of power peaks:

$$\sum_{k=1}^{\frac{n-1}{2}} |E_x(x_k, L_{MMI})|^2 - |E_x(x_{n-k}, L_{MMI})|^2 =$$

$$= \sum_{k=1}^{\frac{n-1}{2}} -4A_0 A_n \cos\left(\frac{\pi}{W} x_k\right) \cos(k\pi) \cos\Delta\phi. \quad (18)$$

Finally, let us define the adimensional parameter I_{odd} as:

$$I_{odd} = \frac{\sum_{k=1}^{\frac{n-1}{2}} |E_x(x_k, L_{MMI})|^2 - |E_x(x_{n-k}, L_{MMI})|^2}{\sum_{\tau=0}^{-n} |E_x(x_{\tau}, L_{MMI})|^2} \Rightarrow$$

$$\Rightarrow I_{odd} = \frac{\sum_{k=1}^{\frac{n-1}{2}} -4A_0 A_n \cos\left(\frac{\pi}{W} x_k\right) \cos(k\pi)}{\sum_{\tau=0}^{n} \left[A_0^2 \cos^2\left(\frac{\pi}{W} x_\tau\right) + A_n^2\right]} \cos\Delta\phi. \tag{19}$$

If n is, now, an even number: there is an odd number of power peaks equal to n+1. The power peak corresponding to $\tau = -\frac{n}{2}$ is the central peak at the origin (x=0) and it is the only one that does not possess a symmetrical one. As before, we may write

$$2A_0 A_n \cos\left(\frac{\pi}{W} x_k\right) \cos\Delta\phi = 2A_0 A_n \cos\left(\frac{\pi}{W} x_{n-k}\right) \cos\Delta\phi$$

but in the case of n even, these terms will present the same sign:

$$|E_x(x_k, L_{MMI})|^2 + |E_x(x_{n-k}, L_{MMI})|^2 =$$

$$= 2A_0^2 \cos^2\left(\frac{\pi}{W}x_k\right) + 2A_n^2 - 4A_0A_n\cos\left(\frac{\pi}{W}x_{n-k}\right)\cos(k\pi)\cos\Delta\phi \quad (20)$$

Adding all the peaks, including the central one, we have

$$\sum_{\tau=0}^{n} |E_x(x_{\tau}, L_{MMI})|^2 =$$

$$= A_0^2 + A_n^2 - 2A_0 A_n \cos\left(\frac{n}{2}\pi\right) \cos\Delta\phi +$$

$$+ \sum_{k=0}^{\frac{n}{2}-1} \left[2A_0 \cos^2\left(\frac{\pi}{W}x_k\right) + 2A_n^2 - 4A_0 A_n \cos\left(\frac{\pi}{W}x_k\right) \cos(k\pi) \cos\Delta\phi \right]. \quad (21)$$

The arguments $\frac{\pi}{W}x_k$ will have the form:

$$\frac{\pi}{W}x_k = \frac{\pi}{W}\left(-k + \frac{n}{2}\right)\frac{W}{n+1} = \frac{n-2k}{n+1}\frac{\pi}{2}.$$

The sum of cosines in Eq. 21, $\sum_{k=0}^{\frac{n}{2}-1} \cos\left(\frac{\pi}{W}x_k\right) \cos(k\pi)$ has an interesting property. Figure 2 shows that the result of this sum alternates between two values, depending on n: $\frac{1}{2}$ and $-\frac{1}{2}$, and we may write

$$\sum_{k=0}^{\frac{n}{2}-1} \cos\left(\frac{\pi}{W}x_k\right) \cos(k\pi) = \sum_{k=0}^{\frac{n}{2}-1} \cos\left(\frac{n-2k\pi}{n+1}\frac{\pi}{2}\right) \cos(k\pi) =$$

$$= \frac{(-1)^{\frac{n}{2}}}{2} = \frac{1}{2}\cos\left(\frac{n\pi}{2}\pi\right) \quad (22)$$

Substituting the result in Eq. 22 in Eq. 21, the result is

$$\sum_{\tau=0}^{n} |E_x(x_{\tau}, L_{MMI})|^2 = A_0^2 + A_n^2 + \sum_{k=0}^{\frac{n}{2}-1} \left[2A_0^2 \cos^2\left(\frac{\pi}{W}x_k\right) + 2A_n^2 \right], \quad (23)$$

which is independent of $\cos \Delta \phi$. Ignoring the central power peak, represented by x_{ψ} , and adding the remaining peaks in the following manner:

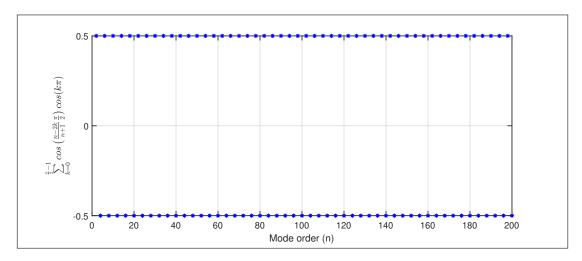


Figure 2. Calculation of the sum in Eq. 22. The values of n are all even non-negative integers. The result alternates between two values: $\frac{1}{2}$ and $-\frac{1}{2}$.

$$|E_x(x_0, LMMI)|^2 - |E_x(x_1, LMMI)|^2 + |E_x(x_2, LMMI)|^2 - \dots + |E_x(x_n, LMMI)|^2 = \sum_{\alpha=0}^{-n} (-1)^{\alpha} |E_x(x_\alpha, L_{MMI})|^2,$$

with $\alpha \in \mathbb{Z}^- + \{0\} - \{x_{\psi}\}$, results in

$$|E_x(x_\alpha, L_{MMI})|^2 = \sum_{\alpha=0}^{-n} (-1)^\alpha \left[A_0^2 \cos^2 \left(\frac{\pi}{W} x_\alpha \right) + A_n^2 \right] - 2A_0 A_n \cos \left(\frac{\pi}{W} x_\alpha \right) \cos \Delta \phi, \quad (24)$$

which is proportional to $\cos \Delta \phi$. Let us, then, define the adimensional parameter I_{even} as:

$$I_{even} = \frac{\sum_{\alpha=0}^{-n} (-1)^{\alpha} |E_x(x_{\alpha}, L_{MMI})|^2}{\sum_{\tau=0}^{-n} |E_x(x_{\tau}, L_{MMI})|^2} \Rightarrow$$

$$I_{even} = \frac{\sum_{\alpha=0}^{-n} (-1)^{\alpha} \left[A_0^2 \cos^2 \left(\frac{\pi}{W} x_{\alpha} \right) + A_n^2 \right] - 2A_0 A_n \cos \left(\frac{\pi}{W} x_{\alpha} \right) \cos \Delta \phi}{A_0^2 + A_n^2 + \sum_{k=0}^{\frac{n}{2} - 1} \left[2A_0^2 \cos^2 \left(\frac{\pi}{W} x_k \right) + 2A_n^2 \right]}$$
(25)

Eqs. 19 and 25 provide expressions that are proportional to $\cos\Delta\phi$ and allow us to

infer the accumulated phase difference between the two modes within the MMI after an arbitrary propagating distance L_{MMI} . One important property of the adimensional parameters I_{odd} and I_{even} , given respectively by Eqs. 19 and 25, is that they are independent of the input power coupled to the MMI device. Denoting the input power coupled to the MMI as A, both A_0 and A_n are related to it, depending on the excitation method employed in the input section of the MMI, and they respect the following relations:

$$\begin{cases}
A_0 = p_0 A \\
A_n = p_n A \\
p_0 + p_n = 1
\end{cases}$$
(26)

Both p_0 and p_n are constants and depend solely on the excitation method, assuming it is invariant with time. Substituting Eq. 26 in Eqs. 19 and 25, we have

$$I_{odd} = \frac{\sum_{k=1}^{\frac{n-1}{2}} -4p_0 p_n \cos\left(\frac{\pi}{W} x_k\right) \cos(k\pi)}{\sum_{\tau=0}^{-n} \left[p_0^2 \cos^2\left(\frac{\pi}{W} x_\tau\right) + p_n^2\right]} \cos\Delta\phi,\tag{27}$$

$$I_{even} = \frac{\sum_{\alpha=0}^{n} (-1)^{\alpha} \left[p_0^2 \cos^2 \left(\frac{\pi}{W} x_{\alpha} \right) + p_n^2 \right] - 2p_0 p_n \cos \left(\frac{\pi}{W} x_{\alpha} \right) \cos \Delta \phi}{p_0^2 + p_n^2 + \sum_{k=0}^{\frac{n}{2} - 1} \left[2p_0^2 \cos^2 \left(\frac{\pi}{W} x_k \right) + 2p_n^2 \right]}.$$
 (28)

Both parameters, I_{odd} and I_{even} are independent of the input power, A, and suffer no influence from fluctuations in it. It is also important to note that the same analysis is valid for TM modes, as one only needs to exchange the E_x for the E_y field in Eq. 1 and the demonstration is straightforward.

3. Examples of application of the method

In sensing applications, for instance, the phase difference between the two propagating modes is an information often used to infer the characteristics of a solution or analyte of interest [5,7,9,14]. To illustrate how the method can be employed, two examples are presented: one with a Bimodal Waveguide (BiMW) and one with a Trimodal Waveguide (TriMW). In both cases, we assume the excitation of only two modes, the fundamental and the highest order one.

3.1. Bimodal Waveguide - Odd symmetry case

In the Bimodal Waveguide (BiMW), the two propagating modes are the fundamental and the first order ones. The total electric field inside the BiMW can be calculated by Eq. 2 given a few parameters of the waveguide: the core width (W), the propagation

constants of the two modes (β_0 and β_1), and the amplitude of each mode (A_0 and A_1). According to Eqs. 27 and 28, the actual amplitude of each mode in not necessary, but only the proportion of the input field coupled to each (p_0 and p_1). If we substitute L_{MMI} in Eq. 2 by z, then the expression give the total electric field as a function of the distance z. Figure 3 shows the propagation of the electric field inside the BiMW and the excerpts present the electric field amplitude for a few regions of interest. The BiMW has $W = 3\mu m$, operating wavelength (λ) of 1550 nm, core refractive index of 1.47, and it is assumed that the amplitude of both modes is the same. The propagating constants can be calculated by [18]:

$$\beta_m = \sqrt{k^2 n_1^2 - (2u_m/W)^2},\tag{29}$$

where $k = 2\pi/\lambda$ and n_1 is the refractive index of the waveguide core.

In a practical application, to determine the phase difference between the modes, one would have to measure the intensity of the electric field in the positions given by Eq. 5. Since the highest order mode is the TE₁, we fall in the case where n is an odd number and we utilize Eq. 19 to calculate the adimensional parameter I_{odd} . It is important to remember that I_{odd} provides a value that is proportional to the cosine of the phase difference between the mode at the distance where the e-field intensities have been measured. Figure 4 compares the value of I_{odd} as a function of the distance with the actual phase difference between the modes (represented by $cos(\Delta\phi)$). It is evident that, although they might not be exactly the same, the curves are proportional and the information of $\Delta\phi$ can be obtained from the adimensional parameter proposed by Eq. 19.

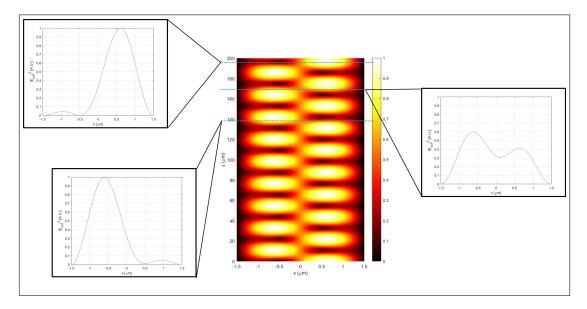


Figure 3. Light propagation within a BiMW with $L_{MMI}=200~\mu m,~W=3~\mu m,~n_1=1.47,$ and operating wavelength $\lambda=1550$ nm. The excerpts show the field amplitude at different distances of the waveguide.

In the context of optical sensing, the idea is not to measure the electric field intensity at several points inside the MMI, but to measure at the end of the waveguide (at the distance $z = L_{MMI}$). Before the test subject (which can be a solution, analyte, temperature, etc.) is inserted in the sensing area, the phase difference between the

modes will have a certain value. After the introduction of the test subject, the power measurements will change due to the perturbation of the propagating modes, rendering a new phase difference between them, which, in turn, is relatable to the change in the refractive index in the sensing area.

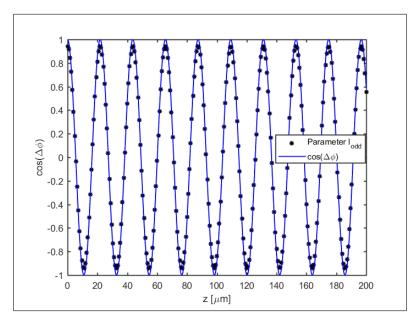


Figure 4. Comparison of the cosine of the actual phase difference $(\Delta \phi)$ between the modes in the BiMW and the calculated parameter I_{odd} .

3.2. Trimodal Waveguide - Even symmetry case

To exemplify the application of the method in a case with even symmetry, a Trimodal Waveguide (TriMW) is presented. Using the same methodology employed for the BiMW, the light propagation in a TriMW with $W=5~\mu m,\,n_1=1.47$ and $\lambda=1550$ nm was studied. Once more, there are only two propagating modes, TE₀ and TE₂, both excited with the same power. Propagation constants, β_m , can be calculated using Eq. 29 and the results can be seen in Figure 5, which presents the propagation through the MMI with total length $L_{MMI}=200~\mu m$.

According to Eq. 5, the TE₂ mode has order n=2, which yields three points with maximum electric field intensity. Measuring the intensity of the total field in these positions throughout the length of the MMI, the adimensional parameter I_{even} can be calculated using Eq. 25. I_{even} provides a quantity that is proportional to the cosine of the phase difference between the TE₀ and TE₂ modes at a given distance. Figure 6 presents both the actual cosine of the phase difference between TE₀ and TE₂ modes and the calculated I_{even} parameter as a function of the propagated distance z. It can be observed that both curves are proportional and the value of $\Delta \phi$ can be acquired from the calculated parameter. Measuring directly a phase difference between two modes may be a complex task, but the presented method allows this information to be obtained by a simple process of measuring field intensity in n specific locations, where n is the order of the higher order propagating mode in the MMI.

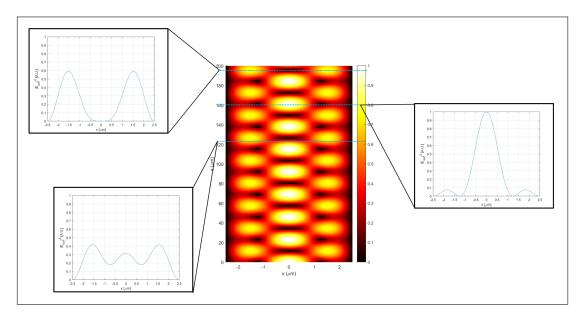


Figure 5. Light propagation within a TriMW with $L_{MMI}=200\mu m,\,W=5\mu m,\,n_1=1.47$, and operating wavelength $\lambda=1550$ nm. The excerpts show the field amplitude at different distances of the waveguide.

4. Conclusion

In summary, in a MMI with solely two propagating modes (fundamental and an arbitrary higher-order modes), the analytical method presented allows the calculation of the phase difference between the two modes at the end of the MMW section. The ability of measuring this phase difference, combined with recent techniques for controlled excitation of modes in MMIs, opens a new range of possible applications for this type of structure, cementing it as an important building block in the field of photonics.

Disclosure statement

The author declares no conflict of interest.

Funding

This work was supported by brazilian agency Fundação de Amparo à Pesquisa de Minas Gerais - FAPEMIG (under process number APQ-00822-19).

References

- [1] Babaki J, Nazari F. Solid-liquid modulator via phononic crystal-based mach-zehnder interferometer. The European Physical Journal Plus. 2022;137(1):1–8.
- [2] Xiao H, Han X, Jiang Y, et al. Demonstration of various optical directed logic operations by using an integrated photonic circuit. Optics Letters. 2021;46(10):2457–2460.
- [3] Al Noman A, Dash JN, Cheng X, et al. Mach-zehnder interferometer based fiber-optic nitrate sensor. Optics Express. 2022;30(21):38966–38974.

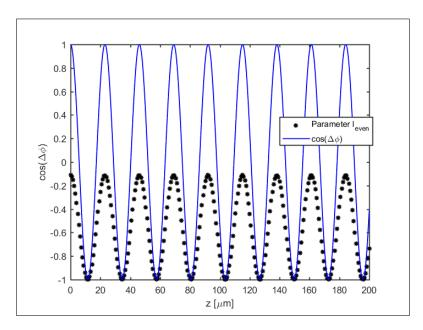


Figure 6. Comparison of the cosine of the actual phase difference $(\Delta \phi)$ between the modes in the TriMW and the calculated parameter I_{even} .

- [4] Laplatine L, Fournier M, Gaignebet N, et al. Silicon photonic olfactory sensor based on an array of 64 biofunctionalized mach-zehnder interferometers. Optics Express. 2022; 30(19):33955–33968.
- [5] Ramirez JC, Gabrielli LH, Lechuga LM, et al. Trimodal waveguide demonstration and its implementations as a high order mode interferometer for sensing application. Sensors. 2019;19(12):2821.
- [6] Hoppe N, Föhn T, Diersing P, et al. Design of an integrated dual-mode interferometer on 250 nm silicon-on-insulator. IEEE Journal of Selected Topics in Quantum Electronics. 2016;23(2):444-451.
- [7] González-Guerrero AB, Maldonado J, Dante S, et al. Direct and label-free detection of the human growth hormone in urine by an ultrasensitive bimodal waveguide biosensor. J Biophotonics. 2017;10(1):61–67.
- [8] Dwivedi R, Kumar A. Refractive index sensing using silicon-on-insulator waveguide based modal interferometer. Optik. 2018;156:961–967.
- [9] Grajales D, Gavela AF, Domínguez C, et al. Low-cost vertical taper for highly efficient light in-coupling in bimodal nanointerferometric waveguide biosensors. Journal of Physics: Photonics. 2019;1(2):025002.
- [10] Ebihara K, Uchiyamada K, Asakawa K, et al. Trimodal polymer waveguide interferometer for chemical sensing. Japanese Journal of Applied Physics. 2019;58(6):062005.
- [11] Liang Y, Zhao M, Wu Z, et al. Investigation of grating-assisted trimodal interferometer biosensors based on a polymer platform. Sensors. 2018;18(5):1502.
- [12] Torrijos-Morán L, Griol A, García-Rupérez J. Slow light bimodal interferometry in one-dimensional photonic. Light: Science & Applications. 2021;10(1):1–12.
- [13] Ramirez JC, Lechuga LM, Gabrielli LH, et al. Study of a low-cost trimodal polymer waveguide for interferometric optical biosensors. Optics Express. 2015;23(9):11985–11994.
- [14] Isayama YH, Hernández-Figueroa HE. High-order multimode interferometer for optical biosensing applications. Sensors. 2021;21(9):3254.
- [15] Isayama YH. Design and numerical demonstration of a multimode interference sensor using engineered slot-waveguides. Optical and Quantum Electronics. 2024;56(3):304.
- [16] Isayama YH, Hernández-Figueroa HE. Design of a novel hybrid multimode interferometer operating with both te and tm polarizations for sensing applications. Optical and

- Quantum Electronics. 2023;55:454.
- [17] Isayama YH. Multimode slot-waveguide sensor using te/tm polarizations for enhanced sensitivity. Sensing and Imaging. 2023;24(1):21.
- [18] Okamoto K. Fundamentals of optical waveguides. 2nd ed. Academic Press; 2006.